

WiLife: Long-term Wi-Fi based Human Daily Status Monitoring with Applications in Eldercare

SHENGJIE LI, Peking University, China and JD.com, China

ZHAOPENG LIU, Peking University, China

QIN LV, University of Colorado Boulder, USA

YANYAN ZOU, JD.com, China

YUE ZHANG, Peking University, China

DAQING ZHANG, Peking University, China

Supporting the global aging population necessitates continuous monitoring of their daily in-home activities, identification of their lifestyle patterns and physical well-being, and prompt detection of anomalies such as insomnia and reduced mobility. While recent research has explored the use of ubiquitous Wi-Fi signals to recognize human behavior, these approaches have been limited to specific activities within controlled environments, such as fall detection within a single room or hand gesture recognition in a fixed location. In response to this limitation, this paper introduces a groundbreaking Wi-Fi-based framework, termed WiLife, designed to provide long-term care by monitoring fundamental aspects of human daily life. These aspects are encapsulated in a triple unit format comprising *(Time, Area, State)*, offering insights into when and where specific activities occur and their associated states. To capture this daily life status information comprehensively, we propose a strategy of partitioning living spaces into functional *areas* and breaking down daily activities into atomic *states*. WiLife, a long-term daily life status monitoring platform, has been successfully implemented and deployed across multiple real-world environments. The analytical findings based on 45×24 hours of daily life status data showcase the system's remarkable ability to infer individuals' living habits and effectively identify abnormal situations. Furthermore, WiLife has been field-tested in a nursing home for an extended period of over a year, where it has been instrumental in providing daily monitoring and detecting anomalies for 22 elderly individuals with Alzheimer's disease.

CCS Concepts: • Human-centered computing → Ubiquitous and mobile computing systems and tools.

Additional Key Words and Phrases: Wi-Fi, Wireless sensing, health monitoring, elderly care

ACM Reference Format:

Shengjie Li, Zhaopeng Liu, Qin Lv, Yanyan Zou, Yue Zhang, and Daqing Zhang. 2018. WiLife: Long-term Wi-Fi based Human Daily Status Monitoring with Applications in Eldercare. *Proc. ACM Meas. Anal. Comput. Syst.* 37, 4, Article 111 (August 2018), 24 pages. <https://doi.org/XXXXXX.XXXXXXX>

1 INTRODUCTION

As global population undergoes a rapid aging process, the population of empty-nest elderly individuals continues to increase [41]. Providing adequate eldercare for these empty-nest elderly poses substantial challenges for many

Authors' addresses: Shengjie Li, lishengjie_java@126.com, Peking University, Beijing, China, lishengjie@JD.com and JD.com, Beijing, China; Zhaopeng Liu, liuzp@pku.edu.cn, Peking University, Beijing, China; Qin Lv, qin.lv@colorado.edu, University of Colorado Boulder, Boulder, CO, USA; Yanyan Zou, zoe.yyzou@gmail.com, JD.com, Beijing, China; Yue Zhang, zhangyue.pro@gmail.com, Peking University, Beijing, China; Daqing Zhang, dqzhang@sei.pku.edu.cn, Peking University, Beijing, China.

Permission to make digital or hard copies of all or part of this work for personal or classroom use is granted without fee provided that copies are not made or distributed for profit or commercial advantage and that copies bear this notice and the full citation on the first page. Copyrights for components of this work owned by others than ACM must be honored. Abstracting with credit is permitted. To copy otherwise, or republish, to post on servers or to redistribute to lists, requires prior specific permission and/or a fee. Request permissions from permissions@acm.org.

© 2018 Association for Computing Machinery.

2476-1249/2018/8-ART111 \$15.00

<https://doi.org/XXXXXX.XXXXXXX>

countries, especially in light of limited healthcare resources.¹. One promising solution to address these challenges is the emerging concept of "*aging-in-place*", where elderly individuals are enabled to maintain their independence and continue residing in their own homes comfortably². However, for empty-nest elderly individuals who live alone, it can pose a significant challenge for their relatives and friends to discern the deterioration of their physical condition. Moreover, in the event of an accident at home, these elderly individuals may lack the capability to assist themselves [6]. Studies have shown that the delay of medical treatment after an accident can increase the mortality risk in some clinical conditions, half of elderly people who experienced an extended period of lying on the floor ($>1\text{h}$) died within six months after the incident [45]. Thus, delivering healthcare support for these aging-at-home empty-nesters has evolved into a pressing social challenge. The crux of addressing this challenge rests in the continuous monitoring of their daily behaviors, promptly detecting abnormalities, and taking appropriate interventions.

In pursuit of the goal of monitoring daily behaviors, numerous systems have been proposed, leveraging technologies such as wearable sensors [13, 27, 32], ambient devices [11, 23], or cameras [8, 48]. However, these approaches are not practical due to various limitations, such as always-worn requirement, deployment complexities, a high rate of false alarms, and privacy concerns. Recently, with the widespread deployment of Wi-Fi infrastructure, Wi-Fi based contactless sensing solutions have been developed [22, 29, 30, 43, 44], enabling human activity sensing in a ubiquitous and privacy-preserving fashion. For empty-nesters eldercare, one straightforward approach is using Wi-Fi based activity recognition methods to capture daily activities of the elderly. Unfortunately, existing activity recognition methods operate under the assumption that dedicated static intervals precede and follow each activity [20, 22], simplifying the segmentation of individual activity from a sequence of continuous activities. Moreover, most of these methods require model retraining or calibration whenever environmental factors change, such as the relocation or reconfiguration of furniture or Wi-Fi devices. As a result, current Wi-Fi-based activity recognition systems are not well-suited for the long-term care of the elderly.

Harnessing the potential of ubiquitous Wi-Fi signals, this paper redefines the fundamental nature of at-home eldercare and address the associated challenges from a fresh perspective. One crucial insight lies in the understanding that the living habits and health conditions of the elderly are closely related to spatio-temporal change patterns in their behavioral states. For instance, behaviors such as eating on schedule, regular bathroom use, regular walking, and sufficient sleep serve as indicators of the elderly maintaining healthy lifestyles. Conversely, a sudden decrease in activity or frequent nighttime bathroom visit may signify health deterioration or the emergence of abnormal conditions [38]. Inspired by this insight, rather than attempting to discern detailed activities, we focus on recognizing coarse-grained activity states of the individual being monitored (hereinafter referred to as the "state") and formulate the problem as continuous monitoring of an elder person's daily spatio-temporal life status (i.e., $\langle \text{Time}, \text{Area}, \text{State} \rangle$). However, in practice, obtaining such spatio-temporal life status is challenging due to the following reasons:

- **Precise positioning of functional areas.** Understanding the precise area in which the target is located, such as the kitchen or bathroom, provides crucial semantic context for monitoring the daily life status of at-home elderly individuals. The precise positioning of functional areas (e.g., bedroom vs. bathroom) requires accurately determining which side of the area boundary line the target is located on. However, with a 90-th percentile localization error of 2 meters [15], traditional Wi-Fi based localization systems struggle to precisely pinpoint the specific functional area where the target is situated.
- **Abstraction and distinction of behavioral states.** In addition to identifying spatial areas, it is equally crucial to ascertain the activity states within a specific area at a given time to depict the daily life status accurately. However, the elderly can carry out a variety of rich daily activities in their daily lives, including eating,

¹"World population ageing: 2020" (the United Nations)

²"Aging in Place: US State Survey of Livability Policies and Practices"

sleeping, watching TV, cooking, etc. The challenge at hand is how to abstract these activities into several enumerable behavioral states and then effectively differentiate between these behavioral states using Wi-Fi.

Our work is dedicated to addressing these two technical challenges in order to facilitate long-term daily status monitoring of the elderly and make following contributions:

- We propose to utilize the walls and its extensions as well-defined boundaries, which naturally divided the whole space into several functional areas (e.g., kitchen, bedroom, bathroom). By continually determining whether a person is inside or outside multiple wall boundaries of a house, we can consistently acquire precise area information about the sensing target.
- Regarding the distinction of behavioral states, we have observed that diverse activities can be categorized based on the movement range of activities, which can be abstracted into three kinds of high-level behavioral states: still, walking, and in-situ moving. By utilizing the Doppler effect to detect the range of movement, we can effectively segment continuous moving activities into these three distinct atomic states.
- Leveraging these spatio-temporal segmentation technologies, an individual's daily life status can be represented as a series of triple units following the format of $\langle \text{Time}, \text{Area}, \text{State} \rangle$. Building upon these two methods, we have developed WiLife, a long-term daily life status monitoring platform, and showcased its effectiveness in capturing daily life habits and anomalies through real-world deployments.

A demonstration video of our spatio-temporal segmentation methods and the WiLife website can be accessed online³. Presently, WiLife is deployed in a nursing home to monitor the living habits and detect abnormal situations of 22 Alzheimer's patients.

2 WILIFE

2.1 Platform Overview

As shown in Figure 1, the WiLife platform mainly consists of three modules: 1) space segmentation module, 2) state segmentation module, and 3) daily life status mining module.

The space segmentation module aims at drawing clear lines (i.e., sensing boundary) to divide the home space into several functional areas (e.g., kitchen, bedroom) and then determines whether a human target has entered a functional area or not, obtaining the current ***Area*** information of the target.

The state segmentation module aims at segmenting the continuous activities into atomic states (i.e., ***still, in-situ moving, walking***). In-situ moving refers to actions that are taken in the same position. Based on above two modules, at a certain ***Time***, we can get the target daily life status, i.e., the triple unit $\langle \text{Time}, \text{Area}, \text{State} \rangle$.

The daily life status mining module is designed to accumulate the long-term records of such daily life status, and further mine the daily habits of the target, where a habit vector can be constructed to characterize the 24-hour life in a day. Then in order to quantify the regularity of daily life on a certain day, a living index is further extracted based on the habit vector. More importantly, by observing the changes of such an index, abnormal situations can be also captured in time.

2.2 Basis for Wi-Fi Sensing

The Wi-Fi settings often consist of a pair of transmitter and receiver. The signal received at the receiver is a superposition of signals propagating from direct paths and reflected paths (i.e., reflected by the human, wall and other objects), namely multi-path propagation. Thus, the received signals also convey information that characterizes the effects of human presence in the environment. If we consider the physical space (including ambient objects and human) as a wireless channel, the Wi-Fi Channel State Information (CSI) depicts the effects when the wireless

³<https://youtu.be/4HDolTd6hbk>

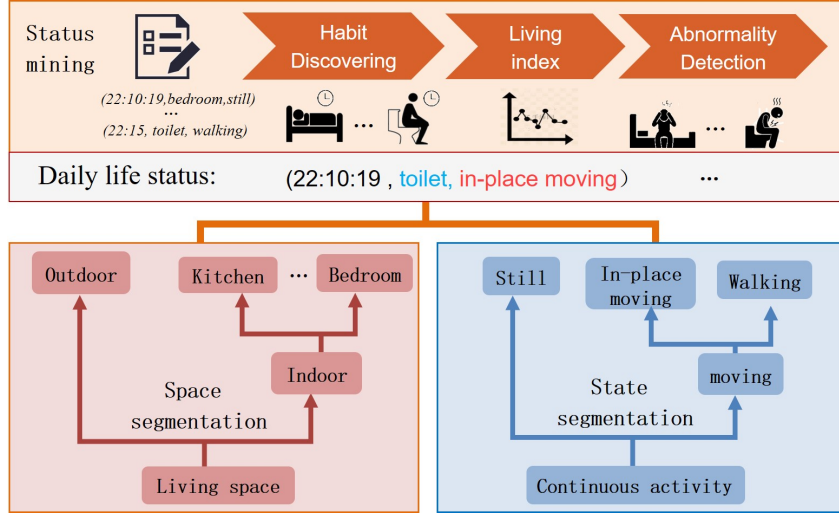


Fig. 1. Overview of WiLife. (the WiLife platform mainly consists of three modules: a space segmentation module, a state segmentation module, and a daily life status mining module.)

signals pass through this wireless Channel [17]. As a consequence, the CSI can be expressed as [47]:

$$H(f, t_0 + t) = e^{j\theta_{offset}} (A_s e^{j\phi_s} + \sum_{d=1}^D \alpha_d(t_0 + t) e^{j\phi_d(t_0 + t)}) \quad (1)$$

where $e^{j\theta_{offset}}$ is random phase offset due to asynchronous hardware, $A_s e^{j\phi_s}$ is merged static signal (i.e., reflected by static objects such as walls or furniture), d is the number of human reflected signals, $\tau_d(t_0 + t)$ is the propagation delay of the d -th signal at time $t_0 + t$, $\alpha_d(t_0 + t)$ is the amplitude attenuation,

After applying conjugate multiplication between CSI on two antennas to eliminate the random phase offset [31], we can derive a new conjugate-multiplying CSI as shown in Equation 2.

$$H_1(f, t_0 + t) \cdot H_2^*(f, t_0 + t) = \underbrace{A_{s_1} A_{s_2} e^{j(\phi_{s_1} - \phi_{s_2})}}_1 + \underbrace{\sum_{d=1}^D \alpha_d(t_0) e^{-j(\phi_d^1(t_0 + t) + \phi_{s_1})}}_2 + \underbrace{\sum_{d=1}^D \alpha_d(t_0) e^{j(\phi_d^2(t_0 + t) - \phi_{s_2})}}_3 \quad (2)$$

The new conjugate-multiplying CSI is composed of three components, where the first component is a constant and does not change over time, and the second and the third components (i.e., including human reflected signals) would change corresponding to the human target movement.

2.3 Segmentation of Spatial Location

To achieve the segmentation of spatial location, the key observation is that the amplitude of signals directly reflected by a person (i.e., direct signals) attenuates gradually in an open space, while the signal amplitude attenuates dramatically when the person moves behind a wall (i.e., direct signals become indirect through-wall signals), as illustrated in Figure 2a.

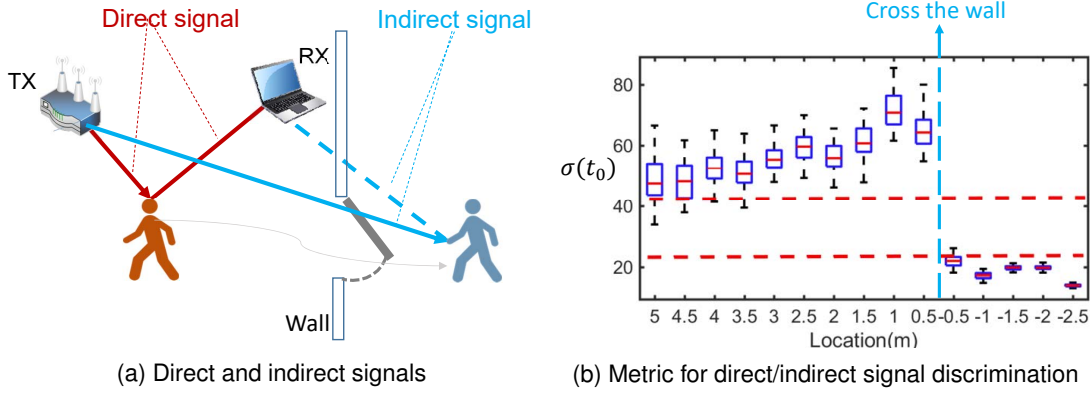


Fig. 2. (a) Illustration of direct and indirect signals when human moves inside-wall and outside-wall respectively; (b) the basic boundary sensing feature for inside-wall and outside-wall signal discrimination.

To characterize such signal amplitude for inside-wall and outside-wall discrimination, a metric $\sigma(t_0)$ can be obtained by applying mean-subtract and Rayleigh Fitting operation on conjugate-multiplying CSI [31]:

$$\sigma(t_0) = \sqrt{(A_{s_1}^2 + A_{s_2}^2) \sum_{d=1}^D \alpha_d^2(t_0)/2} = \sqrt{\frac{1}{2M} \sum_{k=1}^M |x(f, t_0 + \Delta t_k)|^2} \quad (3)$$

where M is a set of conjugate-multiplying CSI samples within a short-time window, and $x(f, t_0 + \Delta t_k)$ is the k_{th} sample after subtracting the mean from the set M . As shown in Figure 2b, with Wi-Fi devices deployed inside the room, crossing the wall boundary (i.e., moving from inside the wall to outside the wall) would result in a sudden decrease in the value of $\sigma(t_0)$. Such a sudden change of $\sigma(t_0)$ can thus be utilized to identify the sensing boundaries as defined by walls in residential settings.

Based on the basic boundary sensing feature $\sigma(t_0)$, we here present how to fully take advantage of the $\sigma(t_0)$ extracted from multiple devices to achieve the space segmentation in a multi-room house. For a typical home environment, we can employ multiple existing Wi-Fi transceiver pairs and indoor walls to divide the indoor space into several sub-areas as shown in Figure 3. When the human target moves from one area to another, the direct/indirect signals from different transceivers change due to changes in wall blockage. Suppose the sensing target wants to move from the living room to the bedroom, the target need to move close to the bedroom door (i.e., the boundary between the living room and the bedroom). As shown in Figure 4a, when he/she gets close to the door but is still outside the bedroom, $RX3$ and $RX4$ receive direct signals, while other devices receive indirect signals. Right after he/she crosses the door and enters the bedroom, no direct signals reach $RX3$ or $RX4$ due to the blockage of the bedroom walls. Only $RX1$ receives direct signals as shown in Figure 4b.

By extracting $\sigma(t_0)$ metrics from each receiver, we are able to obtain the direct/indirect signal situations of all receivers. If we encode the situations of having indirect or direct signals as 0 or 1 to each receiver, then an area transition diagram can be constructed offline as shown in Figure 5. For example, the indirect/direct signal encoding of the scenario in 4a can be represented as ($RX1=0, RX2=0, RX3||RX4=1, RX5=0$) (i.e., 0010) where “||” refers to “or”. When the encoding becomes ($RX1=1, RX2=0, RX3||RX4=0, RX5=0$) (i.e., 1000) in 4b, the system will be triggered to update the area state of the sensing target as “inside the bedroom” as the new encoding matches one entry of the predefined transition encoding. Thus, once we have gathered real-time 0/1 encoding from all receivers, we can accurately determine a target person’s area using the Area-Transition-Diagram.

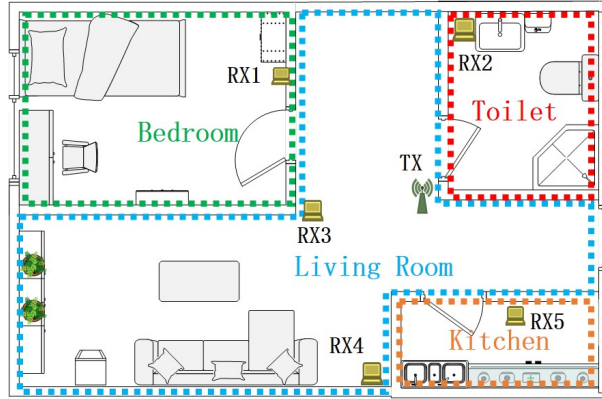


Fig. 3. Space segmentation with one transmitter and multiple receivers.

2.4 Segmentation of Continuous States

Next, we describe how WiLife segments the continuous state sequence. Given a pair of Wi-Fi transmitter (TX) and receiver (RX), the path length of the human reflected signal (i.e., TX \Rightarrow Human \Rightarrow RX) changes when the person is moving, which introduces the phase change of conjugate-multiplying CSI, whose phase $\phi_d^1(t_0 + t)$ in Equation 2 can also be expressed as:

$$\phi_d^1(t_0 + t) = 2\pi f(\tau_{t_0} + \frac{v_D t}{c}) \quad (4)$$

f is the carrier frequency of the signal. c is the light speed, and the v_D is the path length change speed of the human reflected signal, named as *Doppler velocity*. Then utilizing the phase analysis on conjugate-multiplying CSI [34], we can obtain the Doppler velocity v_D to characterize the human movement. As shown in Figure 6, the value of v_D is zero when the target is still and non-zero when the target is moving. Considering a person's daily life states, they can be divided into three categories: (1) still state when the person is mostly stationary such as sleeping; (2)

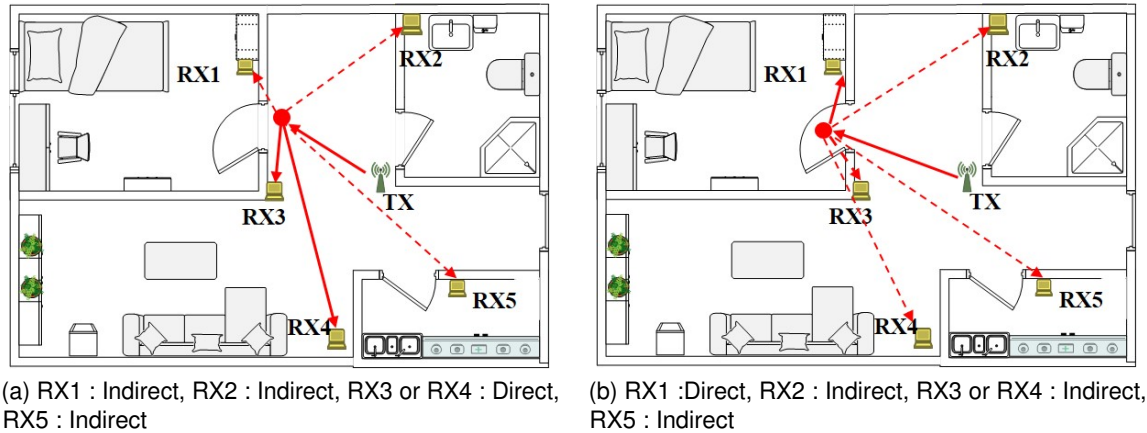


Fig. 4. Direct/indirect signal situations on receivers when people move in different sub-areas.

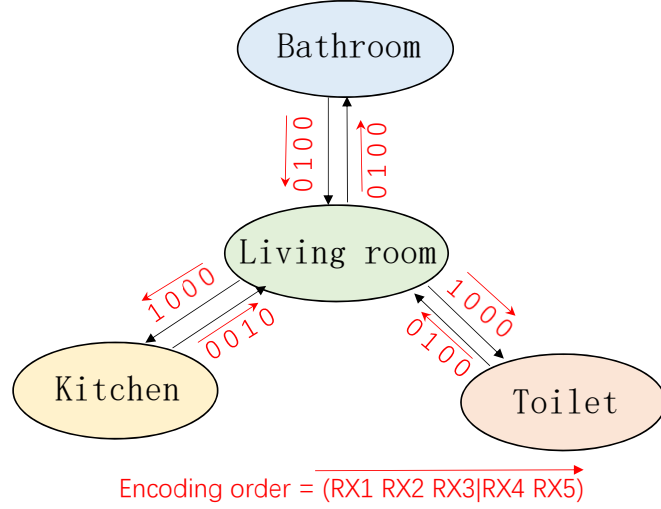


Fig. 5. Area-Transition-Diagram (the system updates the area state only if the new encoding matches one entry of the predefined transition encoding. Otherwise, it remains the area state unchanged).

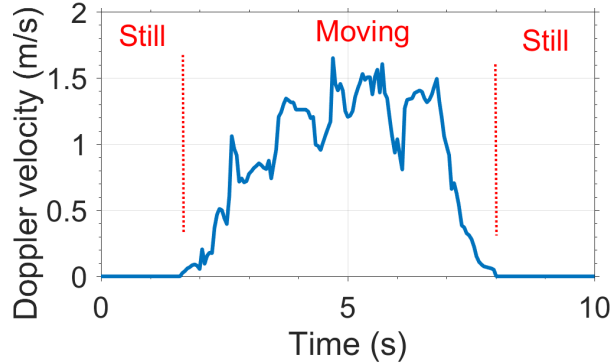


Fig. 6. Obtained Doppler velocity (the value of Doppler velocity is zero when the target is still and non-zero when the target is moving).

in-situ moving state when the person is doing in-situ activities like cooking; and (3) walking state when the person is walking, like moving from a bedroom to a bathroom. The still state can be easily determined when the Doppler velocity is zero. The challenge is distinguishing between the walking and in-situ moving states. We observe that the in-situ moving states often occur in specific locations (e.g., cooking by the stove), where the position of the person changes irregularly in a small range. In contrast, the walking state would introduce a certain displacement in a certain direction, and the range of position changes is relatively large and regular. Based on this observation, we can use the Doppler velocities extracted from all receivers to obtain the approximate maximum displacement of the target in a short time window:

$$\max_{\text{Dis}}(t) = \max_{i=1}^N \int_{t-\Delta t}^t \frac{v_{D_i}}{2} dt, \quad (5)$$

where N is the number of receivers, and v_{D_i} is the Doppler velocity calculated from the i_{th} receiver. To illustrate the maximum displacement of different activities, a volunteer has performed a series of short-term daily activities, and the corresponding changes of displacement are illustrated in the right sub-figure of Figure 7. The displacement corresponding to the still state is zero, while the one corresponding to the walking state is significantly larger than that of the in-situ moving state. Therefore, the segmentation of continuous states can be performed according to the magnitude of the maximum displacement.

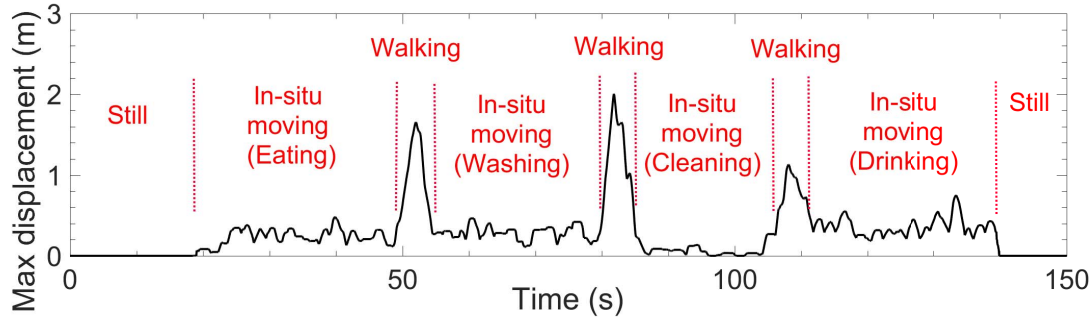


Fig. 7. Maximum displacement of different activities (the displacement corresponding to the still state is zero, while the one corresponding to the walking state is significantly larger than that of the in-situ moving state.)

2.5 Daily Life Status Mining

2.5.1 Overall description. Using the spatio-temporal segmentation methods described above, we can obtain the long-term records of triple units (i.e., \langle Time, Area, State \rangle) to characterize the personal daily life status. For instance, the 24-hour daily life status of a volunteer can be expressed as a radar chart shown in Figure 8. The different colors in the middle of the radar chart represent different functional areas, and the color changes over time indicate the area switching of the sensing target. The periphery of the radar chart shows the maximum displacement change over time, among which the long burr (> 1) is the walking time, the non-burr ($= 0$) is the still time, and the short burr ($0 < \& < 1$) is the in-situ moving time. Such 24-hour overall description demonstrates changes in the volunteer's 24-hour area and state over time. For example, he went out twice, from 7:30am to 8:30am, and from 18:00 to 22:00. When he was indoor, he stayed in the bedroom (colored in green) most of the time, and the infrequent area switching is often accompanied by walking. This example illustrates how we can identify a person's living habits based on the areas and states information. Then, we will dig out the living habits of volunteers from areas and states, respectively.

2.5.2 Bedroom habits. Figure 9 shows the real-life bedroom state change of two volunteers in five days. We mark the longest continuous time in the bedroom as dark green. At a high level, we can see that Volunteer1 spent more time in the bedroom than Volunteer2. However, the temporal distribution of Volunteer1 in the bedroom is relatively scattered, while the time spent by Volunteer2 in the bedroom is relatively concentrated. By reviewing the ground-truth video (camera recording), we found that both volunteers have the habit of working in the bedroom during the day, so the total time in the bedroom is longer. Since Volunteer1 (male) is more active and takes more breaks during work, his time in the bedroom is relatively scattered. In contrast, Volunteer2 (female) has a sedentary habit, and only gets up and leaves the bedroom when she goes to the bathroom or drinks water, so her time in the bedroom is relatively concentrated. Furthermore, when combined with the actual timestamps, we can see that the longest time period in the bedroom basically coincides with the sleep time. Therefore, it can be inferred that the bedtime of Volunteer1 is around midnight and the wake-up time is around 8:00am. In contrast, Volunteer2

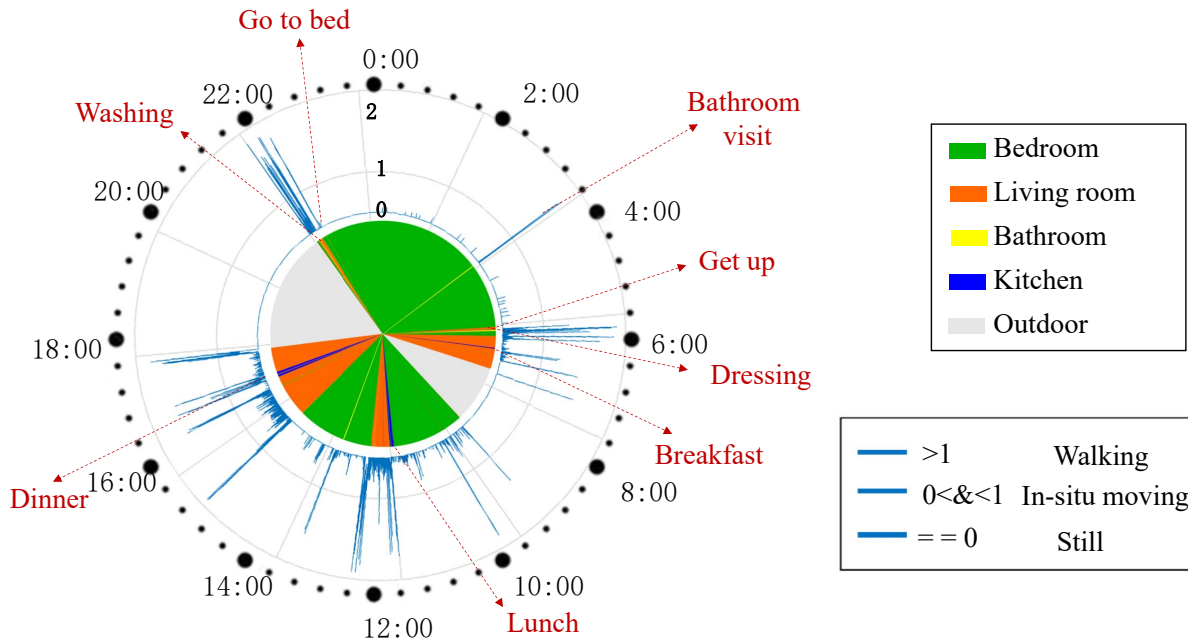


Fig. 8. One volunteer's daily life status over 24 hours (the different colors in the middle of the radar chart represent different functional areas, and the color changes over time indicate the area switching of the sensing target. The periphery of the radar chart shows the maximum displacement change over time, among which the long burr (> 1) is the walking time, the non-burr ($= 0$) is the still time, and the short burr ($0 < & < 1$) is the in-situ moving time).

sleeps later than Volunteer1, usually going to bed around 01:00am and waking up between 8:00am and 9:00am. Zooming in further, we observe a white line between 4:00am and 6:00am during Volunteer1's sleeping period, which actually corresponds to the volunteer's habit of getting up at night. Moreover, if a person has insomnia or dreams a lot at night, his/her movement would increase significantly during sleep. Therefore, by checking the movement information during sleep, our platform can also infer sleep quality. Figure 10 shows the time of body movement of the two volunteers during the sleeping period, indicating that both volunteers sleep normally.

2.5.3 Bathroom habits. Similarly, the real-life bathroom state change of two volunteers in five days are shown in Figure 11. In general, Volunteer1 appeared in the bathroom more often than Volunteer2. Examining the width of the red lines, we can identify periods of longer time span in the bathroom. Combined with the time clock, we can infer that these time periods may correspond to the volunteers' bowel movements, which are also verified by the volunteers. As demonstrated by the volunteers' data analysis results, our system can infer participants' bowel movement patterns in terms of time and duration, which can be particularly useful for eldercare.

More broadly, the frequency and duration of participants' bathroom use can reflect important health information. For example, how often a person goes to the bathroom every day reveals his/her body's metabolism. Therefore, our platform counts the total number of times each participant goes to the bathroom in a day and the total amount of time spent in the bathroom, as shown in Figure 12. It can be seen that the number of times the two volunteers go to the bathroom each day is within a reasonable range. Volunteer1 goes to the bathroom more frequently than Volunteer2, while Volunteer 2 spends relatively more time in the bathroom than Volunteer1.

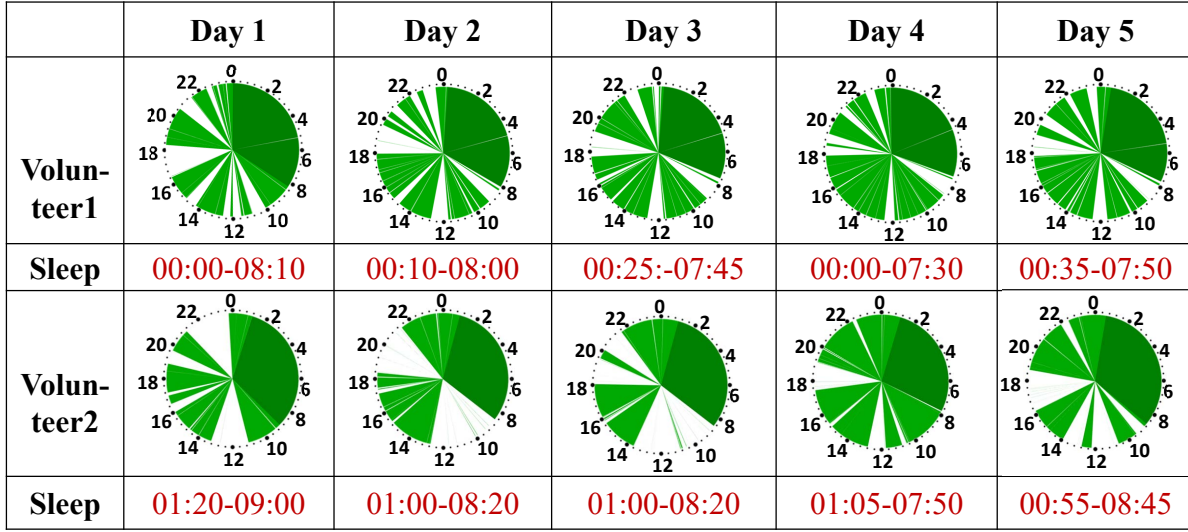


Fig. 9. Bedroom status over time (the real-life bedroom state change of two volunteers in five days. The longest continuous time in the bedroom is marked as dark green. We can see that Volunteer1 spent more time in the bedroom than Volunteer2).

2.5.4 Kitchen habits. Cooking (and sometimes eating) often occurs in the kitchen. Regular entry and exit of the kitchen (dining room) are closely related to the periodicity of eating. Figure 13 shows the kitchen status of two volunteers over time for 5 days. The most obvious blue line in the figure indicates that the volunteers were in the kitchen for a relatively long time. Combined with the time clock, we can infer that these blue lines correspond to the volunteers' three meals in a day. From the multi-day display, we can see that Volunteer1 has the habit of

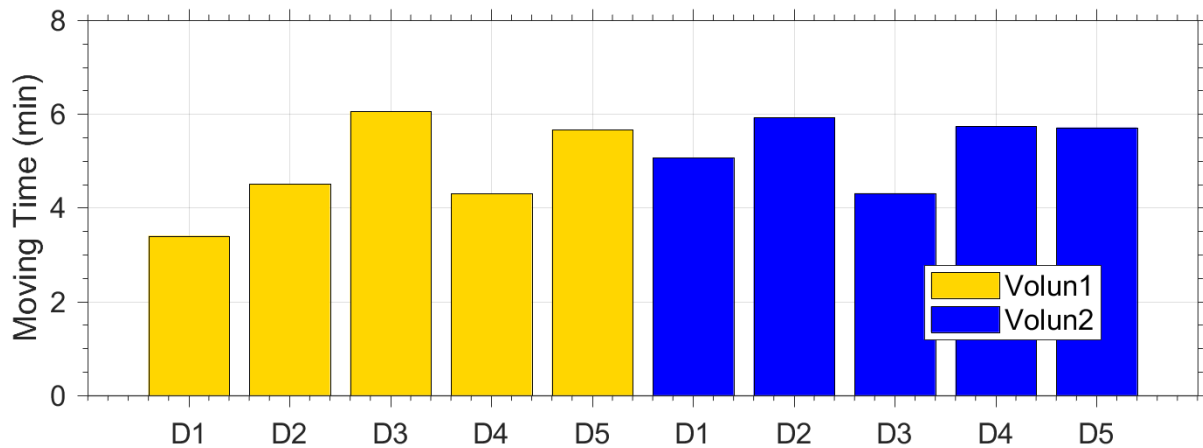


Fig. 10. Total time of moving during sleep. (the figure shows the time of body movement of the two volunteers during the sleeping period, indicating that both volunteers sleep normally).

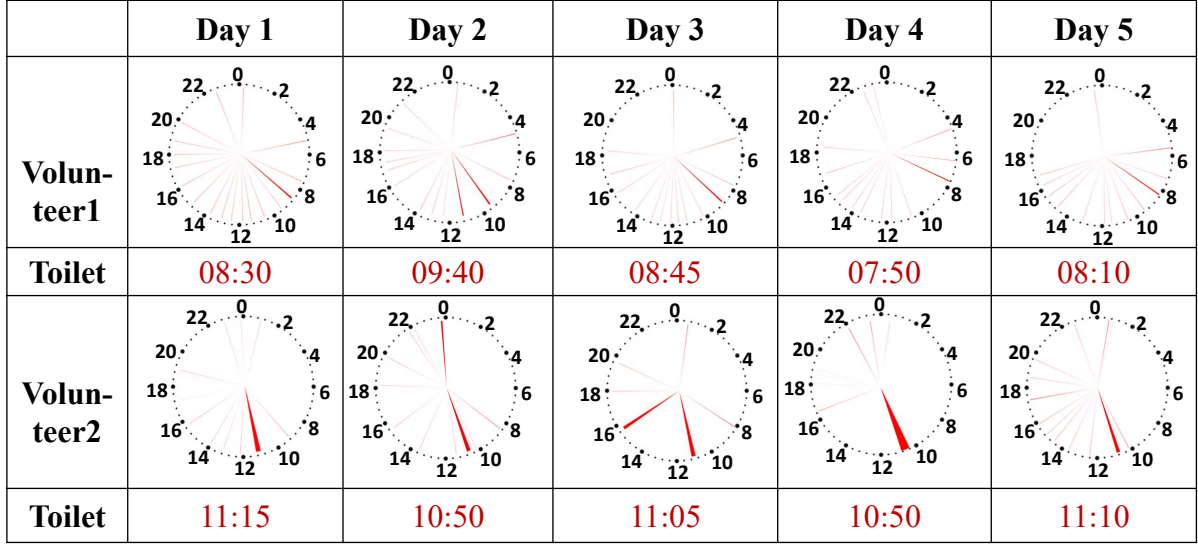


Fig. 11. Bathroom status over time (volunteer1 appeared in the bathroom more often than Volunteer2. Combined with the time clock, we can infer that long time span may correspond to the volunteers' bowel movements).

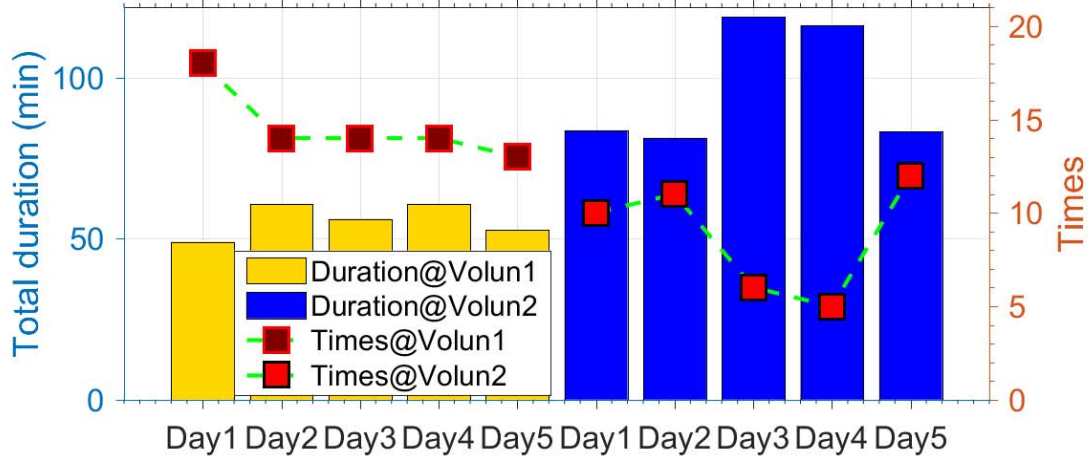


Fig. 12. Number of times and duration in the bathroom (the number of times the two volunteers go to the bathroom each day is within a reasonable range. Volunteer1 goes to the bathroom more frequently than Volunteer2, while Volunteer 2 spends relatively more time in the bathroom than Volunteer1).

eating lunch (around noon) and dinner (between 18:00 and 19:00) at home. In contrast, Volunteer2 only has a late lunch between 12:30 and 13:00.

2.5.5 Human vitality. Our analysis above has revealed the relationship between daily habits (i.e., daily life status) and the area information. Furthermore, the state information is closely related to human life habits and physical health. The daily moving states (in-situ moving and walking) of the elderly reflect their basic daily vitality

	Day 1	Day 2	Day 3	Day 4	Day 5
Volunteer1					
Lunch Dinner	12:25 19:10	12:15 18:35	12:25 18:25	12:00 18:25	12:20 18:40
Volunteer 2					
Lunch	12:50	12:25	13:10	12:30	13:35

Fig. 13. Kitchen status over time (the most obvious blue line in the figure indicates that the volunteers were in the kitchen for a relatively long time. Combined with the time clock, we can infer that these blue lines correspond to the volunteers' three meals in a day).

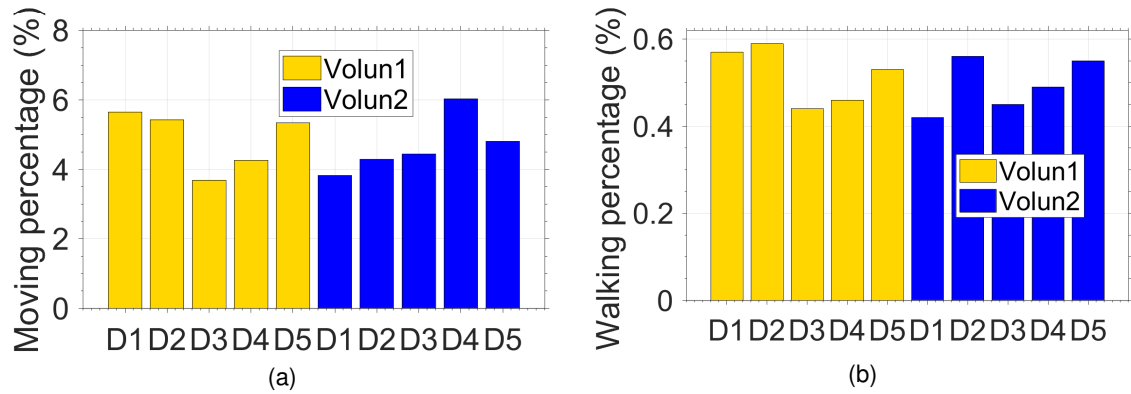


Fig. 14. Percentage of moving (a) and walking time (b). The two volunteers spent most of the day in a still state, and only about 5% of their time is spent on moving while walking time is even less.

level [35], and the walking state is related to the motion ability of the elderly. Therefore, the proportions of moving time and walking time in a day are important indicators to measure an elder's daily vitality. Figure 14 shows the percentage values, we can see that the two volunteers spent most of the day in a still state, and only about 5% of their time is spent on moving while walking time is even less.

Vector	The way of extraction	Meaning
23:00	The start time of the longest and highest proportion of the bedroom time period (after merge short interval)	Approximate time to sleep
08:00	The start time of the longest bedroom time period (after merging short interval) && this period has highest proportion of the still state	Approximate time to get up
4(min)	The total moving during above sleep period	Moving time during sleep (Sleep quality)
05:00	Time of first bathroom visit during above sleep period	First wake up time at night
1	Times of bathroom visit during above sleep period	Times for bathroom at night
10:00	Start time of the longest bathroom period && this period has highest proportion of still state	Start time of toileting
4(min)	Start time of the longest bathroom period with the highest proportion of still state	Duration of toileting
16	Total times of bathroom visit	Times of using bathroom
09:15	Start time of in-situ state in the kitchen for more than 10 minutes && Before 10:00	Breakfast
12:30	Start time of in-situ state in the kitchen with a duration of more than 10 minutes && Between 11:00-15:00	Lunch
18:40	Start time of in-situ state in the kitchen with a duration of more than 10 minutes && Between 16:00-20:00	Dinner
6(%)	Moving time percentage during the day(07:00-23:59)	Basic vitality
0.5(%)	Walking time percentage during the day(07:00-23:59)	Vitality

Fig. 15. Feature extraction of living habits.

2.5.6 Living index. By analyzing the daily life status captured by WiLife, we have unearthed a series of important features about the target life habits. Combined with long-term daily life status and expert knowledge, we can construct a habit vector to describe the target's 24-hour life condition as shown in Figure 15.

After accumulating daily life status records for multiple days, we can extract a habit vector for each day and construct a habit matrix as Equation 6. Since a habit (e.g., bedtime) may vary among different days, each dimensional variable in C follows a normal distribution with corresponding mean and variance values,

$$C = \begin{bmatrix} 00 : 00 & 00 : 10 & \cdots & 00 : 35 \\ 08 : 10 & 08 : 00 & \cdots & 07 : 50 \\ \vdots & \vdots & \ddots & \vdots \\ 0.57 & 0.59 & \cdots & 0.53 \end{bmatrix} \quad (6)$$

When the target starts a new day, we can describe the regularity of the new day's living status based on the similarity between the habit matrix and the habit vector of the new day. Since Mahalanobis distance [37] is applicable to variables with different measures or sample distributions, we use Mahalanobis distance to quantify the similarity between the new habit vector X and the habit matrix C , referred to as *living index*:

$$\text{LivingIndex} = \frac{\epsilon}{(X - m)^T \cdot C^{-1} \cdot (X - m)}, \quad (7)$$

where ϵ is a fixed constant, X is the habit vector corresponding to the new day, C is the habit matrix, m is the mean vector of C , and $(X - m)^T \cdot C^{-1} \cdot (X - m)$ represents the calculation of Mahalanobis distance. A larger *LivingIndex* between X and C means that the new day's living status is more consistent with the daily living habits and patterns, reflecting a more regular and healthy condition.

2.5.7 Anomaly detection. Based on the characteristics of the normal distribution of each variable in the habit matrix in Section 3.5.6, we have generated a series of habit vectors under normal status through simulation.

The habit vectors are divided into two groups. One group of vectors are used to form the habit matrix, and the remaining vectors are used for testing. For the test vector, we change each feature in the vector one by one to simulate the abnormality of the elderly by making the value of the feature deviate from the normal range. Then we comprehensively consider the living index of all normal and abnormal conditions, and use a simple binary classifier to obtain the discrimination threshold (i.e., $livingIndex = 0.5$). For example, Figure 16a shows the living index for several test vectors. When we change the number of wake-ups on the fifth day from 1 (average 1 time) to 4 times, the value of the living index will drop significantly below threshold, as shown in Figure 16b, indicating an abnormal day.

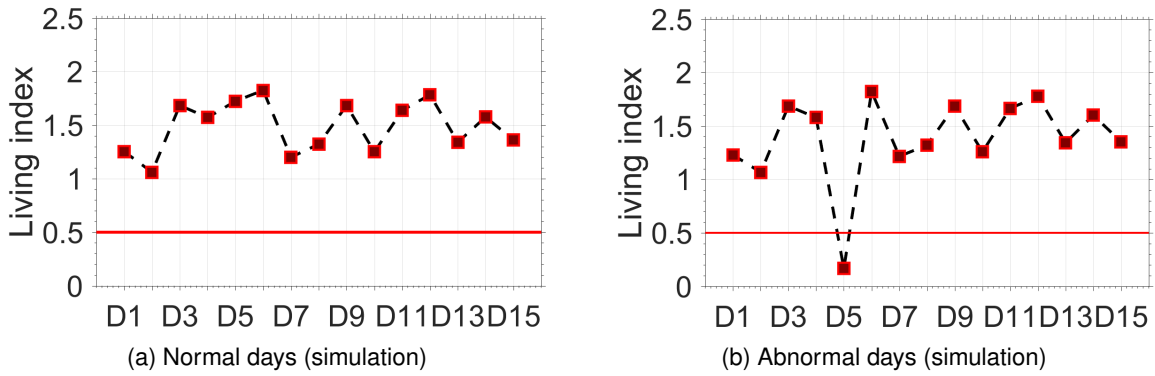


Fig. 16. (a) Living index of normal 15 days (simulation); (b) Living index with an abnormal day (simulation). We can set $livingIndex = 0.5$ as the threshold (red line) to successfully distinguish between normal and abnormal days.

When anomalies are detected, we can further determine the reason. Specifically, it is necessary to calculate the normalized distance between the habit vector of the abnormal day and all samples of the habit matrix as follows:

$$fDist_i = \frac{(fvalue_i - \mu)^2}{\sigma_i^2}, \quad (8)$$

where $fvalue_i$ is the value of the i_{th} feature in the habit vector of the abnormal day, μ and σ^2 are the mean and variance values of the i_{th} feature corresponding to the habit matrix. A larger normalized distance $fDist_i$ means there is a higher probability that the i_{th} feature caused (or contributed to) the abnormality of that day.

3 EVALUATION

3.1 Deployment guidelines

Since the space segmentation module of WiLife leverages the walls or walls' extension to divide the space into different areas, the existence of walls plays an important role in WiLife deployment. WiLife makes use of the walls or walls' extension as the sub-area boundaries. For different layouts in different environments, the signal blockage condition usually differs. As such, we need some guidance in terms of where to place the Wi-Fi transceivers given specific indoor layout, either theoretically or empirically. Assume a space is divided by a common wall into two parts: inside-wall area and outside-wall area, wherein the inside-wall area serves as the sensing zone. Then, in order to leverage the wall or its extensions as a sensing boundary, the following two guidelines are summarized:

- (1) The Wi-Fi receiver is preferably deployed in the inside-wall area and not visible by a sensing target in the outside-wall area.

- (2) The Wi-Fi transmitter can be deployed either in the inside-wall area or outside-wall area, but it should be visible by a human target in the inside-wall area.

Based on the above guidelines, we can quickly select the appropriate places to deploy the transmitter and receivers, as shown in Figure 17a, colored in blue and red. As for multi-room houses, it is also able to achieve multi-boundaries determination based on these two guidelines. As shown in Figure 17b, by reasonably deploying one transmitter and multiple receivers, the multiple boundaries can be formed by multiple walls in the house.

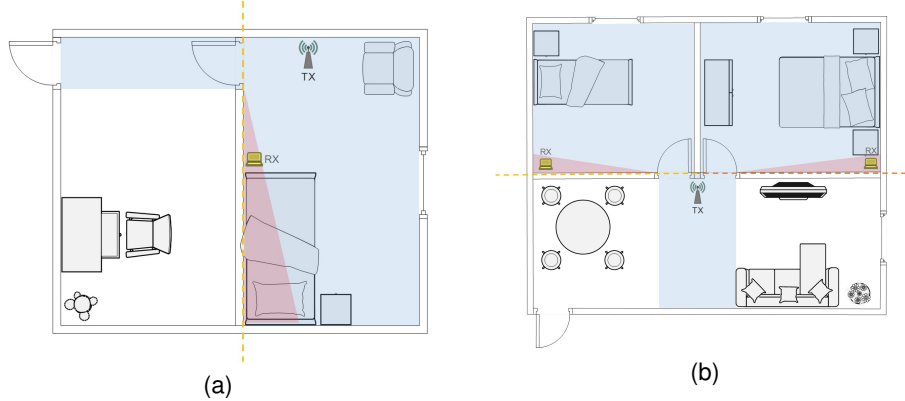


Fig. 17. (a) transceivers deployment for single-boundary determination: blue area for transmitter deployment and red area for receiver deployment; and (b) transceivers deployment for multiple-boundary determination: blue area for transmitter deployment and red area for receivers deployment.

3.2 Evaluation Setup

To evaluate the performance of the WiLife platform, Gigabyte mini-PCs equipped with cheap off-the-shelf Intel 5300 Wi-Fi cards are used for the Wi-Fi transmitter and the receiver. Two antennas are attached to the receiver, and one to the transmitter. We use the CSI Tool developed by Halperin [18] to collect Wi-Fi CSI samples. Both the transmitter and receivers work on the 5GHz band with a 20MHz channel. Based on the deployment guidelines, the WiLife platform is deployed in two real home environments: Smart Home A and Smart Home B. Figure 18 shows the layouts of these two smart homes. The user interface of the platform is presented in Figure 19, from which we can see the real-time Wi-Fi sensing results and ground-truth video. In practical applications, cameras are not required. WiLife has been deployed in a nursing home with 22 Alzheimer's elders for over a year and has been tested by these people, from which we observed that individual diversity has little impact on the performance of WiLife. Due to privacy concerns, we cannot report those results and can only share the test results of another 15 volunteers here to show the robustness and long-term stability of the system in two different environments. Approved by IRB, all volunteers have signed an informed consent form, being aware of the experiment procedures and data usage.

3.3 Evaluation of space segmentation

In both environments, we asked 15 volunteers (5 females, 10 males) to perform daily activities such as cooking, dining, sleeping, watching TV and walking around. During a 20-minute session of activities, volunteers are encouraged to carry out activities while moving across different rooms (as much as possible). It is worthy noting

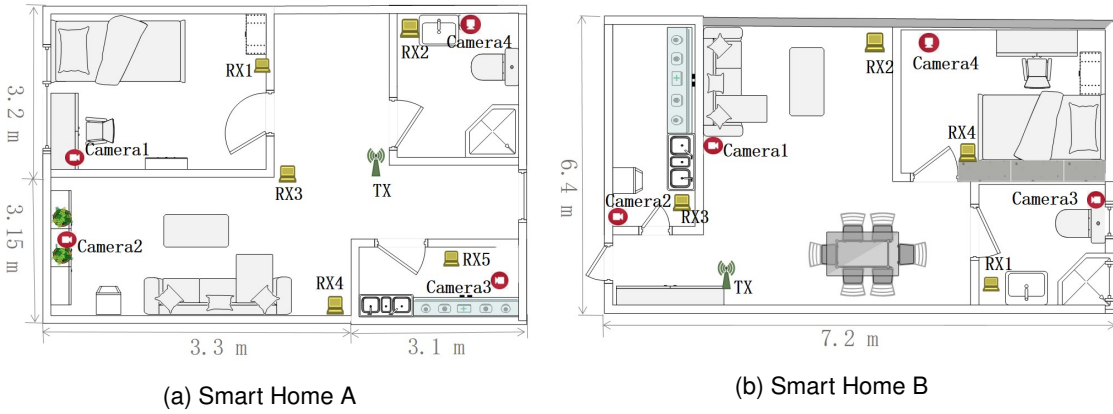


Fig. 18. Experimental environments for WiLife. One Wi-Fi transmitter and five receivers are deployed in smart home A. One Wi-Fi transmitter and four receivers are deployed in smart home B. Multiple Cameras are also deployed to record the ground-truth video. In practical applications, cameras are not required.



Fig. 19. The graphical interface of real-time system, which we can see the real-time Wi-Fi sensing results and ground-truth video.

that no activity instructions are suggested to volunteers, so they can act according to their daily habits. For each volunteer, 15 sessions of activities have been collected, with a total data set of 4500 minutes. These activities were recorded simultaneously by web cameras as ground-truth. During each session of activities, the volunteer can switch to any area or perform any activities as his/her will. In total, 9952 area switches have taken place during the 4500 minutes. The system performance for area detection is presented in the form of confusion matrix, as shown in Figure 20. It is worth noting that there is a transition area in each environment, through which one must pass before reaching another area, e.g., living room in Figure 18. The transition areas suffer from delays in both living room–bedroom and living room–bathroom switches. Hence, their accuracy is slightly lower than that of the

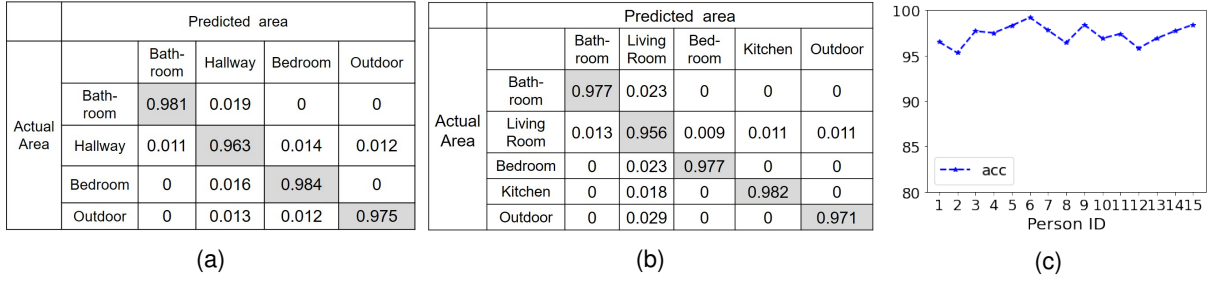


Fig. 20. Space segmentation result: (a) and (b) are confusion matrices for two environments; (c) is accuracy for different participants.

other areas. Also, in the presence of such transition areas, the human target is not able to switch directly between bedroom and bathroom/kitchen. Thus, we can notice that all the mistakes in the confusion matrix are caused by switches between adjacent areas. Apart from the evaluation of different environments, we also evaluate the system against individual diversity, and the system performs consistently for different individuals as shown in Figure 20c. Overall, the space segmentation module achieves a high area detection accuracy of up to 97.3%.

3.4 Evaluation of state segmentation

We also evaluate the performance of the state segmentation module using the data set collected above. In the total data set of 4500 minutes, 30,357 segments of different states are collected, 35% for walking, 20% for in-situ moving, and 45% for the still state. The performance of state segmentation is presented in Figure 21. Like transition areas, in-situ moving plays a role as a transition state. Thus, the walking state is not able to switch directly to the still state, resulting in zero mutual error between these two states. However, since the in-situ moving state can switch to each of the other two states, the accuracy is slightly lower. With regard to individual diversity, the system performances for different people are also consistent, as shown in Figure 21c.

3.5 Evaluation of overall platform

To the best of our knowledge, this is the first work that monitors human daily status naturally and continuously in real-world settings, which prevents us from comparing directly with other baseline methods. To evaluate the overall performance of WiLife, we deployed the system in the above two real-home environments and kept it running

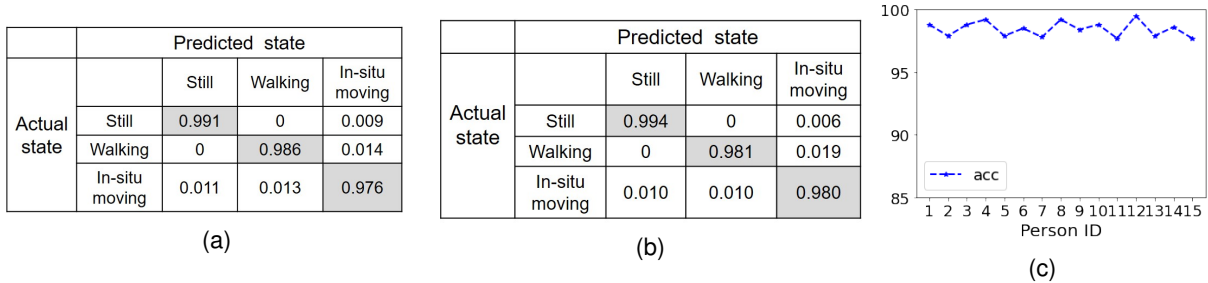


Fig. 21. State segmentation result: (a) and (b) are confusion matrices for two environments; (c) is accuracy for different participants.

continuously throughout the day. We invited three volunteers (see Table 1) to carry out their daily activities in these two homes. Volunteer2 and Volunteer3 each has lived in Smart Home A for 15 days, and Volunteer1 has lived in Smart Home B for 15 days. To record the ground-truth, web cameras were also installed. Moreover, we have built a website to visualize the long-term records of daily life status. The screenshot of the WiLife website is illustrated in Figure 22

Table 1. Information about volunteers. D refers to days.

	Gender	Age	Height	Weight	In A	In B
Volunteer1	male	25	183cm	92kg	—	15D
Volunteer2	femail	27	162cm	53kg	15D	—
Volunteer3	male	34	173cm	70kg	15D	—



Fig. 22. The screenshots of website for data analysis.

To understand the daily habits of the volunteers as soon as possible, we first carefully observed the recorded videos of the volunteers during a normal day, obtaining their daily habit vectors. We further confirmed these daily habits with the volunteers in the form of questionnaires, and learned about the numerical deviations of their habits, thus constructing their habit matrices. Then, the living index can be extracted to characterize the 15×24 hours'

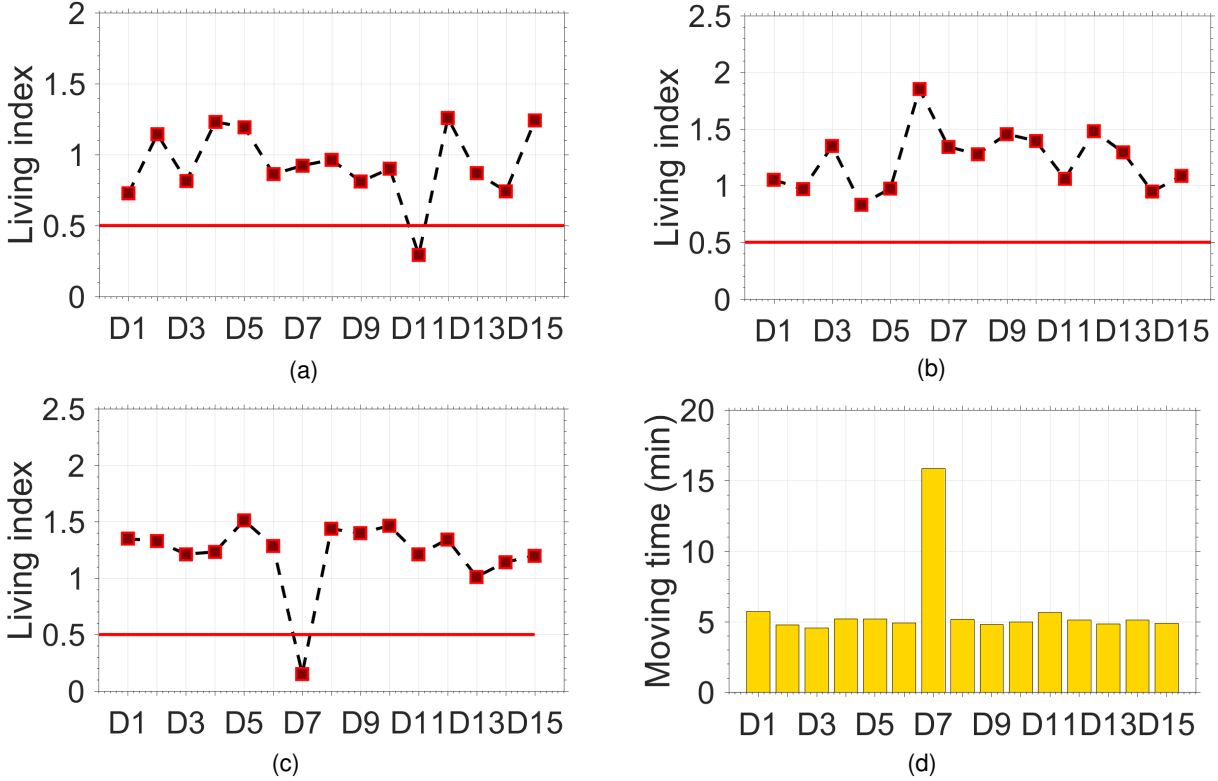


Fig. 23. (a)~(c) are living indices of Volunteer1~Volunteer3; (d) total time of moving during sleep for Volunteer3 on all days. Volunteer1 and Volunteer3 are abnormal on the 11th and 7th day, respectively, while Volunteer2 is normal for all 15 days. The total time of moving during sleep reflects that the volunteer3 suffered from insomnia on the 7th night.

daily life for each volunteer, as shown in Figure 23a~23c. As we can see, Volunteer1 and Volunteer3 are abnormal on the 11th and 7th day, respectively, while Volunteer2 is normal for all 15 days. In addition, considering the overall fluctuation range of the living index, the daily habits of Volunteer3 (except for the abnormal day) is more regular than that of the other two volunteers. To further study the cause of the abnormality, we first extract the habit vector of Volunteer1 on the 11th day and Volunteer3 on the 7th day, and then calculate the normalized distance of each feature in the habit vector. As shown in Figure 24, the normalized distance of Feature12 and 13 on the 11th day of Volunteer1 is relatively large, indicating that these two features are abnormal. Based on the feature definition in the habit vector, these two features represent the percentage of moving and walking time during the day.

Then, we can compare these two features of Volunteer1 for all 15 days. As shown in Figure 25, the values of these two features are significantly lower than other days. After reviewing the ground-truth video, we found that Volunteer1's sitting and lying time increased significantly on the 11th day. Through return visit, we learned that Volunteer1 did get sick on the 11th day, which explains the anomalies and demonstrates the capability of our platform to detect such anomalies. Similarly, for Volunteer3, as shown in Figure 23d, the abnormal feature represents the total time of moving during sleep, which reflects that the volunteer suffered from insomnia on the 7th night.

4 RELATED WORK

Eldercare. The topic of eldercare has attracted increasing attention in elder living and healthcare communities. Various eldercare systems have been proposed [14, 16]. Commonly-used wearable sensors include gyroscopes [27], accelerometer sensors [13], RFIDs [36], smartwatches [24] and smartphones [21]. These solutions require the subject to wear or carry such sensors all the time for continuous monitoring, which is inconvenient. Some people may be willing to sacrifice convenience for finer-grained sensing granularity. However, these techniques can only recognize a single action (e.g., fall) or activities that consist of repeating actions, such as respiration, running, cycling. In daily life, the activities of the elderly can be various. Many activities are irregular and last for a long time, such as cooking and going to the toilet. Even with wearable devices, these complex activities cannot be recognized. On the other hand, due to the accuracy of GPS, wearable devices cannot provide room-level fine-grained location information (where in the home). Therefore, these methods cannot be applied to the long-term daily status monitoring of the elderly. Moreover, for the long-term health monitoring of the elderly, the most important thing is to find abnormal behaviors rather than recognize a specific action. Other systems exploit the ambient information (e.g., audio noise [11], floor vibration [19, 39], infrared sensing data [23, 25]), motion and touching [9] to achieve eldercare in a non-intrusive way. However, these systems require the deployment of dedicated devices in the environment, and sound noise and pressure around the subject in the environment might cause frequent false alarms. Another line of research uses cameras installed in the home environment [8], which is restricted by the line of sight, computation cost for real-time processing, as well as privacy concerns [10]. In terms of using various radars for human sensing, Doppler radar [12] can sense the human moving but it would be difficult to obtain the fine-grained living habit information. FMCW radars [3, 4] require the strict linear relationship between the transmission time and frequency, which is difficult to satisfy in practice. When sensing a large range or sensing through walls, UWB radar [7] requires high instantaneous transmission power and introduces high costs [5]. Such radar-based techniques may work well in specific scenarios, but their current deployments are limited. In contrast, this work leverages Wi-Fi signals that are widely available and also offers good privacy protection. Compared with above sensing technologies, Wi-Fi devices are ubiquitous in indoor environments. Various home Wi-Fi-enabled appliances (e.g., router, TV) form many pairs of Wi-Fi communication links. Extra infrastructures are not required if the existing Wi-Fi signals can be utilized for elderly sensing.

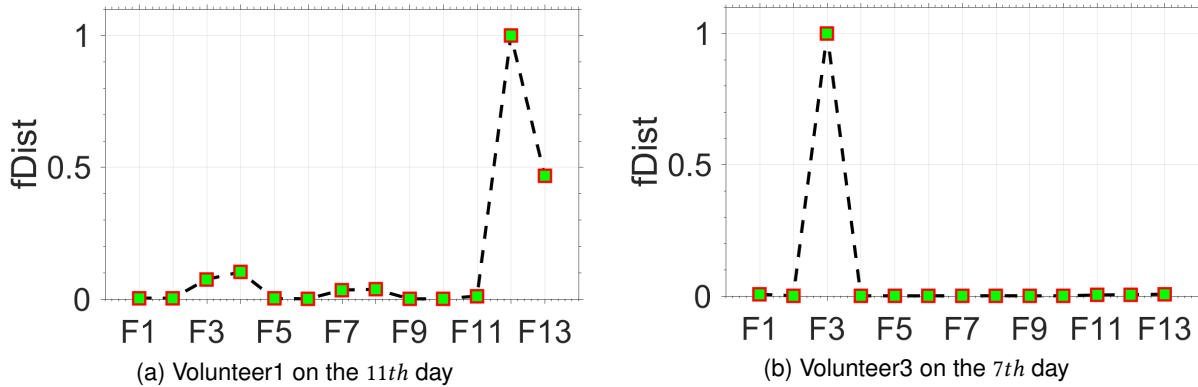


Fig. 24. Distance for features on the abnormal day (F: Feature). The distance of Feature12 and 13 on the 11th day of Volunteer1 is relatively large, which indicate the percentage of moving and walking time during the day.

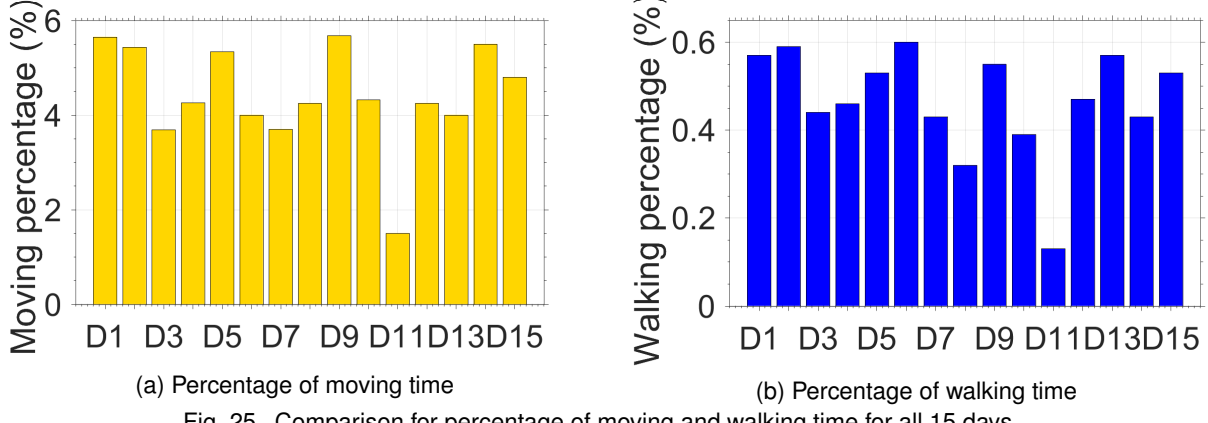


Fig. 25. Comparison for percentage of moving and walking time for all 15 days.

Device-free Sensing using Wi-Fi. Wi-Fi signal has been explored to achieve device-free sensing, with applications for localization and activity recognition [1, 33, 40, 42–44, 46]. Existing Wi-Fi based localization approaches, such as fingerprinting based [1, 42, 46] and geometric-based [26, 33] methods, are sensitive to environmental change or require manual calibration after each device initialization, which limit their application to long-term eldercare. In addition, the 90-th percentile error of existing localization systems is still as high as 2m [15], which hinders their use in real-world home applications. The Wi-Fi signals can also be used for human activity recognition [20, 22, 43, 44], such as fall detection [20], gesture recognition [2, 28], and exercise recognition [29]. Most existing studies [43, 44] perform two steps to achieve activity recognition: activity segmentation and activity classification. The key assumption is that the activity can be manually segmented or there is a set of pre-defined rules on actions (e.g., remaining still before and after an action). Furthermore, the mainstream of activity classification methods are sensitive to the subject’s location and orientation [49]. To function properly, these methods require the user to take actions in a fixed location and even fixed orientation. As such, these methods are not suitable for long-term eldercare in real-world environments.

Instead of recognizing precise location and activity for eldercare, this paper proposes to monitor coarser-grained daily life status, including the Area and State information at a certain time. Correspondingly, we have developed a novel platform based on Wi-Fi sensing technologies to perform continuous monitoring and anomaly detection for eldercare.

5 DISCUSSION

Real-word deployments. Our study has demonstrated the effectiveness of WiLife in real-world deployments. Since WiLife identifies user location when the target enters each room’s door (i.e., boundary line), it is not affected by the size of the room. Also, the activity state segmentation module works within a 10-meters range. Therefore, as long as there are one or two Wi-Fi routers acting as transmitter(s) and one Wi-Fi device in each room acting as receivers, WiLife can work in apartments or homes with different room sizes and different layouts. However, since WiLife leverages the walls or walls’ extension to divide the space into different areas, the main requirement is that the walls should be made of materials which can attenuate RF waves to certain extent. Thus, WiLife may not work well with glass walls or thin wood walls in some houses.

Changes of environments. For long-term (e.g. months or years) monitoring of daily status, we have to take into account changes that may exist in the environments. For both methods of Segmentation of Spatial Location and Segmentation of Continuous State, the static signals in the environment have been removed. In terms of

Segmentation of Spatial Location, the performance is only related to the occlusion of dynamic signals by walls in the environment. In other words, the performance only changes when the relative position between the transceiver and the wall changes drastically. In this case, the model needs to be re-calibrated to fit the change. Therefore, we have developed a lightweight automatic calibration mechanism embedded in the system, which allows users to re-calibrate the system by re-sampling both in-wall and out-wall activities and then the model can be automatically re-calibrated. Response Fig 26 demonstrates a user interface for the activity sampling. For example, if the location of the receiver in the bedroom changes significantly, the user can click the "Start" button (in "in-wall" row, "bedroom" column) to start data collecting, and take a in-wall walk for a while. Then, the user needs to click the "End" button after finish in-wall walking. Similarly, the user can also re-sample an out-wall activity through similar operations. Afterwards, the system can automatically get a new threshold, thus re-calibrating itself successfully.



Fig. 26. User interface for lightweight calibration. For example, to re-calibrate the receiver in the bedroom, the user can click the "Start" button (in "in-wall" row "bedroom" column) to take a in-wall walk for a while, and then end the walk after clicking the "End" button. Similarly, the user can also re-sample an out-wall activity through similar operations. Afterwards, the system will automatically get a new threshold, thus re-calibrating itself successfully.

Multi-person sensing. Passive or device-free sensing of multiple persons is a well-known challenging problem. When there are multiple targets, each non-still target will generate multiple dynamic signals to the receiver, so the signal received at the receiver is a superposition of multiple targets. Due to the small Wi-Fi bandwidth (20MHz), it is extremely difficult for commodity Wi-Fi devices to separate these reflected path signals and obtain the accurate number of targets. This is an important direction for our future work.

Further useful insights. Apart from informing elders' health condition decline and abnormal situations in terms of daily status, WiLife can be further extended to enable applications such as fall detection and sleep monitoring. For example, we interestingly discovered that different sleep stages (Rapid Eye Movement Sleep, Non-Rapid Eye Movement Sleep) are accompanied by different breathing rates and body movements, which can be extracted from Wi-Fi signals, thus allowing for the possibility of fine-grained analysis of sleep conditions. With further advances of Wi-Fi sensing technology, we envision a suite of rich functionalities being developed on top of our WiLife framework for eldercare and other application domains.

6 CONCLUSION

Advances in ubiquitous Wi-Fi technology enable new healthcare options for aging-in-place empty-nest elderly. Utilizing commodity Wi-Fi, this paper proposes to support eldercare via continuous monitoring of daily life status (i.e., ⟨Time, Area, State⟩). Our work is the first that combines the spatial and temporal states of the target. Through the analysis of 45 × 24 hours of daily life status in real-life environments (and deployment in a nursing home), WiLife can effectively infer users' living habits and detect abnormal situations. Future work includes providing richer daily life information and further exploring the daily status monitoring of multiple people.

REFERENCES

- [1] Heba Abdel-Nasser, Reham Samir, Ibrahim Sabek, and Moustafa Youssef. 2013. MonoPHY: Mono-stream-based device-free WLAN localization via physical layer information. In *WCNC*.
- [2] Heba Abdelnasser, Moustafa Youssef, and Khaled A. Harras. 2015. WiGest: A ubiquitous WiFi-based gesture recognition system. In *INFOCOM*.
- [3] Fadel Adib, Zachary Kabelac, and Dina Katabi. 2015. Multi-Person Localization via RF Body Reflections. In *12th USENIX Symposium on Networked Systems Design and Implementation (NSDI 15)*. Oakland, CA, 279–292.
- [4] Fadel Adib, Zach Kabelac, Dina Katabi, and Robert C. Miller. 2014. 3D Tracking via Body Radio Reflections. In *Proceedings of the 11th USENIX Symposium on Networked Systems Design and Implementation (NSDI '14)*. USENIX Association, Seattle, WA, 317–329.
- [5] Abdulrahman Alarifi, AbdulMalik Al-Salman, Mansour Alsaleh, Ahmad Alnafessah, Suheer Al-Hadhrami, Mai A Al-Ammar, and Hend S Al-Khalifa. 2016. Ultra Wideband Indoor Positioning Technologies: Analysis and Recent Advances. *Sensors (Basel, Switzerland)* 16, 5 (May 2016).
- [6] M. Alwan, P.J. Rajendran, S. Kell, D. Mack, S. Dalal, M. Wolfe, and R. Felder. 2006. A Smart and Passive Floor-Vibration Based Fall Detector for Elderly. In *2006 2nd International Conference on Information and Communication Technologies*, Vol. 1. 1003–1007.
- [7] Boyd Anderson, Mingqian Shi, Vincent Y. F. Tan, and Ye Wang. 2019. Mobile Gait Analysis Using Foot-Mounted UWB Sensors. *Proc. ACM Interact. Mob. Wearable Ubiquitous Technol.* 3, 3, Article 73 (Sept. 2019), 22 pages.
- [8] Q. Cai and J. K. Aggarwal. 1998. Automatic Tracking of Human Motion in Indoor Scenes across Multiple Synchronized Video Streams. In *ICCV*.
- [9] Loïc Caroux, Charles Consel, Lucile Dupuy, and Hélène Sauzéon. 2014. Verification of Daily Activities of Older Adults: A Simple, Non-Intrusive, Low-Cost Approach. In *Proceedings of the 16th International ACM SIGACCESS Conference on Computers and Accessibility* (Rochester, New York, USA) (ASSETS '14). Association for Computing Machinery, New York, NY, USA, 43–50. <https://doi.org/10.1145/2661334.2661360>
- [10] George Demiris, Debra Oliver, Jarod Giger, Marjorie Skubic, and Marilyn Rantz. [n. d.]. Older adults' privacy considerations for vision based recognition methods of eldercare applications. *Technology and health care* ([n. d.]).
- [11] Thilina Dissanayake, Takuya Maekawa, Daichi Amagata, and Takahiro Hara. 2018. Detecting Door Events Using a Smartphone via Active Sound Sensing. *Proc. ACM Interact. Mob. Wearable Ubiquitous Technol.* 2, 4, Article 160 (Dec. 2018), 26 pages.
- [12] D. P. Fairchild and R. M. Narayanan. 2016. Multistatic micro-doppler radar for determining target orientation and activity classification. *IEEE Trans. Aerospace Electron. Systems* 52, 1 (2016), 512–521.
- [13] F Foerster, M Smeja, and J Fahrenberg. 1999. Detection of posture and motion by accelerometry: a validation study in ambulatory monitoring. *Computers in Human Behavior* (1999).
- [14] Kathrin Gerling, Mo Ray, Vero Vanden Abeele, and Adam B. Evans. 2020. Critical Reflections on Technology to Support Physical Activity among Older Adults: An Exploration of Leading HCI Venues. *ACM Trans. Access. Comput.* 13, 1, Article 1 (apr 2020), 23 pages. <https://doi.org/10.1145/3374660>
- [15] Wei Gong and Jiangchuan Liu. 2018. SiFi: Pushing the Limit of Time-Based WiFi Localization Using a Single Commodity Access Point. *IMWUT* (2018).
- [16] Abhay Gupta, Kuldeep Gupta, Kshama Gupta, and Kapil Gupta. 2020. A Survey on Human Activity Recognition and Classification. In *2020 International Conference on Communication and Signal Processing (ICCP)*. 0915–0919. <https://doi.org/10.1109/ICCP48568.2020.9182416>
- [17] Daniel Halperin, Wenjun Hu, Anmol Sheth, and David Wetherall. 2011. Tool Release: Gathering 802.11N Traces with Channel State Information. *SIGCOMM Comput. Commun. Rev.* 41, 1 (Jan. 2011), 53–53.
- [18] Daniel Halperin, Wenjun Hu, Anmol Sheth, and David Wetherall. 2011. Tool Release: Gathering 802.11N Traces with Channel State Information. *SIGCOMM Comput. Commun. Rev.* 41, 1 (Jan. 2011), 53–53.
- [19] J. Hamilton, B. Joyce, M. Kasarda, and Pablo Tarazaga. 2014. *Characterization of Human Motion Through Floor Vibration*.
- [20] Chunmei Han, Kaishun Wu, Yuxi Wang, and Lionel M. Ni. 2014. WiFall: Device-free fall detection by wireless networks. In *INFOCOM*.
- [21] Tian Hao, Guoliang Xing, and Gang Zhou. 2015. RunBuddy: A Smartphone System for Running Rhythm Monitoring. In *Ubicomp*.

- [22] Wenjun Jiang, Chenglin Miao, Fenglong Ma, Shuochao Yao, Yaqing Wang, Ye Yuan, Hongfei Xue, Chen Song, Xin Ma, Dimitrios Koutsonikolas, Wenyao Xu, and Lu Su. 2018. Towards Environment Independent Device Free Human Activity Recognition. In *Mobicom*.
- [23] Ju Han and B. Bhanu. 2005. Human Activity Recognition in Thermal Infrared Imagery. In *CVPR*.
- [24] Young-Ho Kim, Diana Chou, Bongshin Lee, Margaret Danilovich, Amanda Lazar, David E. Conroy, Hernisa Kacorri, and Eun Kyoung Choe. 2022. MyMove: Facilitating Older Adults to Collect In-Situ Activity Labels on a Smartwatch with Speech. In *Proceedings of the 2022 CHI Conference on Human Factors in Computing Systems* (New Orleans, LA, USA) (*CHI '22*). Association for Computing Machinery, New York, NY, USA, Article 416, 21 pages. <https://doi.org/10.1145/3491102.3517457>
- [25] Simon Klakegg, Jorge Goncalves, Chu Luo, Aku Visuri, Alexey Popov, Niels van Berkel, Zhanna Sarsenbayeva, Vassilis Kostakos, Simo Hosio, Scott Savage, Alexander Bykov, Igor Meglinski, and Denzil Ferreira. 2018. Assisted Medication Management in Elderly Care Using Miniaturised Near-Infrared Spectroscopy. *Proc. ACM Interact. Mob. Wearable Ubiquitous Technol.* 2, 2, Article 69 (July 2018), 24 pages.
- [26] Manikanta Kotaru, Kiran Joshi, Dinesh Bharadia, and Sachin Katti. 2015. SpotFi: Decimeter Level Localization Using Wi-Fi. In *SIFCOMM*.
- [27] Oscar D. Lara and Miguel A. Labrador. 2013. A Survey on Human Activity Recognition using Wearable Sensors. *IEEE Communications Surveys Tutorials* (2013).
- [28] Hong Li, Wei Yang, Jianxin Wang, Yang Xu, and Liusheng Huang. 2016. WiFinger: talk to your smart devices with finger-grained gesture. In *Ubicomp*.
- [29] Shengjie Li, Xiang Li, Qin Lv, Guiyu Tian, and Daqing Zhang. 2018. WiFit: Ubiquitous Bodyweight Exercise Monitoring with Commodity Wi-Fi Devices. In *UIC*.
- [30] Shengjie Li, Xiang Li, Kai Niu, Hao Wang, Yue Zhang, and Daqing Zhang. 2017. AR-Alarm: An Adaptive and Robust Intrusion Detection System Leveraging CSI from Commodity Wi-Fi. In *ICOST*.
- [31] S. Li, Z. Liu, Y. Zhang, Q. Lv, and D Zhang. 2020. WiBorder: Precise Wi-Fi based Boundary Sensing via Through-wall Discrimination. *IMWUT* (2020).
- [32] Seon-Woo Lee Li and K. Mase. 2002. Activity and location recognition using wearable sensors. *IEEE Pervasive Computing* 1, 3 (July 2002), 24–32.
- [33] Xiang Li, Shengjie Li, Daqing Zhang, Jie Xiong, Yasha Wang, and Hong Mei. 2016. Dynamic-MUSIC: Accurate Device-free Indoor Localization. In *Ubicomp*.
- [34] Xiang Li, Daqing Zhang, Qin Lv, Jie Xiong, Shengjie Li, Yue Zhang, and Hong Mei. 2017. IndoTrack: Device-Free Indoor Human Tracking with Commodity Wi-Fi. *IMWUT* (2017).
- [35] Xiang Li, Daqing Zhang, Jie Xiong, Yue Zhang, Shengjie Li, Yasha Wang, and Hong Mei. 2018. Training-Free Human Vitality Monitoring Using Commodity Wi-Fi Devices. *IMWUT* (2018).
- [36] Yunhao Liu, Yiyang Zhao, Lei Chen, Jian Pei, and Jinsong Han. 2012. Mining Frequent Trajectory Patterns for Activity Monitoring Using Radio Frequency Tag Arrays. *IEEE Trans. Parallel Distrib. Syst.* (2012).
- [37] R. D. Maesschalck, D. Jouan-Rimbaud, and D. L. Massart. 2000. The Mahalanobis distance. *Chemometrics and Intelligent Laboratory Systems* (2000).
- [38] M. G. Marmot, James Banks, R. Blundell, C. Lessof, and James Nazroo. 2003. Health, wealth and lifestyles of the older population in England: The 2002 English Longitudinal Study of Ageing. *PNAS* (2003).
- [39] Robert J Orr and Gregory D Abowd. 2000. The smart floor: a mechanism for natural user identification and tracking. In *CHI '00 Extended Abstracts on Human Factors in Computing Systems*. 275–276.
- [40] Kun Qian, Chenshu Wu, Zheng Yang, Yunhao Liu, and Kyle Jamieson. 2017. Widar: Decimeter-Level Passive Tracking via Velocity Monitoring with Commodity Wi-Fi. In *Proceedings of the 18th ACM International Symposium on Mobile Ad Hoc Networking and Computing* (Chennai, India) (*MobiHoc '17*). ACM, New York, NY, USA, Article 6, 10 pages.
- [41] Teo. 2006. Ageing in Singapore. (2006).
- [42] Ju Wang, Hongbo Jiang, Jie Xiong, Kyle Jamieson, Xiaojiang Chen, Dingyi Fang, and Binbin Xie. 2016. LiFS: Low Human-effort, Device-free Localization with Fine-grained Subcarrier Information. In *Mobicom*.
- [43] Wei Wang, Alex X. Liu, Muhammad Shahzad, Kang Ling, and Sanglu Lu. 2015. Understanding and Modeling of Wi-Fi Signal Based Human Activity Recognition. In *Mobicom*.
- [44] Yan Wang, Jian Liu, Yingying Chen, Marco Gruteser, Jie Yang, and Hongbo Liu. 2014. E-eyes: Device-free Location-oriented Activity Identification Using Fine-grained WiFi Signatures. In *MobiCom*.
- [45] Isaacs B Wild D, Nayak US. 1981. How dangerous are falls in old people at home?. In *Br Med J (Clin Res Ed)*. Article 282, 266-268 pages.
- [46] Kaishun Wu, Jiang Xiao, Youwen Yi, Min Gao, and Lionel M. Ni. 2012. FILA: Fine-grained indoor localization. In *INFOCOM*.
- [47] Zheng Yang, Zimu Zhou, and Yunhao Liu. 2013. From RSSI to CSI: Indoor Localization via Channel Response. *ACM Comput. Surv.* 46, 2, Article 25 (Dec. 2013), 32 pages.
- [48] Xinguo Yu. 2008. Approaches and principles of fall detection for elderly and patient. In *HealthCom 2008*.
- [49] D. Zhang, H. Wang, and D. Wu. 2017. Toward Centimeter-Scale Human Activity Sensing with Wi-Fi Signals. *Computer* (2017).